Co-grinding significance for calcium carbonate-calcium phosphate mixed cement. Part II: effect on cement properties

Solene Tadier, Nadine Le Bolay, Sophie Girod Fullana, Sophie Cazalbou, Cédric Charvillat, Michel Labarrère, Daniel Boitel, Christian Rey, Christèle Combes

Cogrinding significance for calcium carbonate–calcium phosphate mixed cement. II. Effect on cement properties

Solène Tadier,[1] Nadine Le Bolay,[2] Sophie Girod Fullana,[3] Sophie Cazalbou,[3] Cédric Charvillat,[1] Michel Labarrère,[4] Daniel Boitel,[4] Christian Rey,[1] Christèle Combes[1]

[1]Université de Toulouse, CIRIMAT, UPS-INPT-CNRS, ENSIACET, 4, allée Emile Monso, BP 44362, 31030 Toulouse Cedex 4, France
[2]Université de Toulouse, Laboratoire de Génie Chimique, UPS-INPT-CNRS, ENSIACET, 4 allée Emile Monso, BP 44362, 31030 Toulouse Cedex 4, France
[3]Université de Toulouse, CIRIMAT, UPS-INPT-CNRS, Faculté de Pharmacie, 118 Route de Narbonne, 31062 Toulouse cedex 4, France
[4]Université de Toulouse, Institut Clément Ader, INSA-UPS-Mines Albi, ISAE DMSM, 10 Av. Edouard Belin, BP 50032, 31055 Toulouse cedex 4, France

Abstract: In the present study, we aim to evaluate the contribution of the cogrinding process in controlling calcium carbonate-dicalcium phosphate dihydrate cement properties. We set a method designed to evaluate phase separation, usually occurring during paste extrusion, which is quantitative, reliable, and discriminating and points out the determining role of cogrinding to limit filter-pressing. We show that solid-phase cogrinding leads to synergistic positive effects on cement injectability, mechanical properties, and radio-opacity. It allows maintaining a low ($<$0.4 kg) and constant load during the extrusion of paste, and the paste's composition remains constant and close to that of the initial paste. Analogous behavior was observed when adding a third component into the solid phase, especially $SrCO_3$ as a contrasting agent. Moreover, the cement's mechanical properties can be enhanced by lowering the *L*/*S* ratio because of the lower plastic limit. Finally, unloaded or Sr-loaded cements show uniform and increased optical density because of the enhanced homogeneity of dry component distribution. Interestingly, this study reveals that cogrinding improves and controls essential cement properties and involves processing parameters that could be easily scaled up. This constitutes a decisive advantage for the development of calcium carbonate-calcium phosphate mixed cements and, more generally, of injectable multicomponent bone cements that meet a surgeon's requirements. J Biomed Mater Res Part B: Appl Biomater 99B: 302–312, 2011.

Key Words: bone cement, calcium carbonate, calcium phosphate, cogrinding, injectability, radio-opacity

How to cite this article: Tadier S, Bolay N, Fullana S, Cazalbou S, Charvillat C, Labarrère M, Boitel D, Rey C, Combes C. 2011. Cogrinding significance for calcium carbonate–calcium phosphate mixed cement. II. Effect on cement properties. J Biomed Mater Res Part B 2011:99B:302–312.

INTRODUCTION

Injectable bone substitutes and especially fast-setting biomimetic mineral cements have great potential for procedures involving defects with limited accessibility or narrow cavities, when there is a need for the precise placement of the paste and when using minimally invasive surgical techniques. Consequently, injectable systems should shorten surgical operation time, minimize damaging effects on large muscle retraction, reduce scar size, and lessen postoperative pain, allowing patients to achieve rapid recovery in a cost-effective manner. One of the main technological and scientific difficulties encountered during the implantation procedure of injectable calcium phosphate bone cements is the control of viscosity and cohesiveness of the paste, which has to be easily injectable with a syringe and must also set and harden rapidly (in a few minutes) in contact with biological fluids and tissues.[1–4] The two main undesirable phenomena affecting paste cohesiveness that occur during injection and/or at the early contact of the paste with biological fluid are "filter-pressing" (the separation of particulate/powder and liquid within the syringe, resulting in plugging, and partial paste extrusion) and "cement washout" (the disintegration of the paste occurring during the early contact of the paste with biological fluids or tissues).[5–10] It is of prime importance to avoid the occurrence of these phenomena to control the composition and homogeneity of the extruded paste and, consequently, the composition and setting of the cement implanted *in vivo.* Even though the injectability of calcium phosphate cement pastes has been investigated theoretically and experimentally by several authors,[11–18] there are no standard procedures to evaluate paste injectability and cohesiveness (phase separation, paste disintegration . . .). Recently, our group proposed a

Correspondence to: C. Combes; e-mail: christele.combes@ensiacet.fr
Contract grant sponsor: Institut National Polytechnique de Toulouse; contract grant number: BQR INPT 2006

protocol to examine the cement paste injectability based on the measurements of the load required to extrude a given volume of paste and of the weight of paste extruded.[19,20]

Among the various parameters that have been shown to determine cement paste injectability are the solid phase particle morphology, particle mean size, specific surface area, particle size distribution, interparticle interactions, and agglomeration state.[13,16,18,21-24] Most of these parameters can be modified by grinding and cogrinding the reactive powders. Other parameters have also been investigated including the introduction of additives, particle surface charge, liquid to solid (L/S) ratio, and the injection system (syringe) geometry.[7,8,12-15,25] However, little attention has been paid to thoroughly examining the contribution of the cogrinding treatment of the solid phase for multicomponent mineral bone cements.

Another concern of surgeons using such injectable bone substitutes is being able to follow-up the injection and evolution of the cement by radiography. Wang et al.[26] have shown that the introduction of strontium, an oligo-element naturally present in bone, in cement formulation enhances mineral cement radio-opacity, injectability, and mechanical properties of amorphous calcium phosphate-dicalcium phosphate dihydrate (DCPD) bone cement. Other authors have also pointed out the interest in incorporating strontium (as salts, ions, or strontium-substituted reactive powder) in bone cement formulation.[1,4,27-30] Note that the dose-dependent and antagonist effects of strontium on bone mineralization *in vivo* have also been reported.[31,32] In the present study, strontium is used as a contrasting agent but also as a marker of cement homogeneity to determine the role of cogrinding for multicomponent cements.

In part I of this study,[33] an original methodology involving complementary analytical techniques allowed us to thoroughly investigate the grinding mechanism of separated or mixed reactive powders and its consequences on solid phase reactivity and setting ability. We pointed out the antagonist effects cogrinding can have on cement setting: by showing that cogrinding the solid phase leads to a paste that sets earlier (setting time is halved), whereas the progress of the setting chemical reaction involving the dissolution/reprecipitation phenomena is delayed by 30 min, probably because of the increased contact area between the reactive powders limiting their hydration. It is now of interest to investigate in part II the contribution of the cogrinding process on $CaCO_3$-DCPD cement properties.

The objectives of the present study are to examine the contribution of the cogrinding process in controlling $CaCO_3$-DCPD cement properties, particularly cement injectability, mechanical properties, and radio-opacity and to set a protocol to evaluate the phase separation (filter-pressing) usually occurring during mineral paste extrusion.

MATERIALS AND METHODS

Reactive powder syntheses

The reactive powders constituting the solid phase of the cement (DCPD and $CaCO_3$ vaterite) were synthesized by precipitation at room temperature and stored in a freezer following protocols previously described in detail.[34]

Very recently, we showed that, unlike DCPD powder, vaterite powder grinding was inefficient because of the low-initial average particle size close to the size limit (around 2 μm), as also noted for other mineral compounds and cements.[33] However, to investigate the possible role of vaterite powder characteristics, especially on the cement paste injectability, we set a second protocol of vaterite preparation to obtain vaterite powder (called vaterite 2 or V2) with different particle sizes and/or morphologies than the vaterite powder previously prepared and presented[33,34] (the latter is called vaterite 1 or V1). Thus injectability of pastes prepared with solid phase including V1 or V2 will be compared, whereas the other properties will be evaluated only for cements prepared with solid phase including V1.

V2 was prepared at room temperature by double decomposition between a calcium chloride solution (0.5 mol in 250 ml of deionized water) and a sodium carbonate solution (0.5 mol in 500 ml of deionized water). The calcium solution was added to the stirred carbonate solution using a peristaltic pump (flow rate of 25 ml/min). Then, the precipitate was rapidly filtered and washed with 1.5 L of deionized water. After filtration and washing, the precipitate was lyophilized and the as-synthesized powder (50 g) stored in a freezer.

Commercial strontium carbonate (Alfa Aesar®) was used as a source of strontium for cement solid phase formulation. $SrCO_3$ has solubility close to that of $CaCO_3$, which is already present in the cement; consequently, $SrCO_3$ should be resorbable and should not significantly modify the behavior of this cement in aqueous medium.

Reactive powder treatment by grinding or cogrinding

Dry batch grinding and cogrinding experiments were performed using a laboratory tumbling ball mill in order to reach the smallest particle size and good powder mixture as recently described in detail by Tadier et al.[33] Briefly, it consisted of a 1-L alumina ceramic cylindrical chamber rotating around its horizontal axis and containing alumina ceramic balls of three different diameters: 19, 9.2, and 5.6 mm. The rotating speed of the chamber was fixed at 100 rpm, that is, at 75% of the critical speed, while the ball loading volume represented 40% of the whole volume of the chamber: the volume ratio of balls of each size was 1/2 for 19 mm balls, 1/4 for 9.2 mm balls, and 1/4 for 5.6 mm balls. The powder filling rate (10 g) represented 2% of the void space between the balls. DCPD powder was ground separately or coground with vaterite powder. In the latter case, a 1:1 weight ratio of DCPD and vaterite powder mixture constituted the solid phase for $CaCO_3$-DCPD cement preparation was coground. Powder samples were taken from different regions of the mill chamber at various times to be analyzed. The sample mass removed at each time was small enough (0.5% w/w) to not modify significantly the powder proportion in the mill. Immediately after removal, the particle size distribution of the samples, expressed as volume, was determined using a dry laser diffraction granulometer (Malvern Mastersizer 2000), and the median size, $d_{0.5}$, corresponding to a cumulated volume percentage of 50%, was determined. These measurements were performed in triplicate in order to check the

reproducibility (on different batches) of these powder treatments. Grinding and cogrinding processes were stopped just before powders began to agglomerate to reach the smallest mean size. The optimum grinding or cogrinding duration has already been determined for DCPD and (DCPD + V1) powders by Tadier et al.[33]: 27 and 13 min, respectively.

All the synthesized and commercial powders were characterized before and after grinding treatment by transmission FTIR spectroscopy from KBr pellets (Nicolet 5700 spectrometer, ThermoElectron), X-ray diffraction (Inel CPS 120 diffractometer) using a Co anticathode ($\lambda = 1.78897$ Å), dry laser diffraction granulometry (Malvern Mastersizer 2000), and scanning electron microscopy (LEO 435 VP microscope; sample silver plating before observation).

Paste preparation and characterization

Paste preparation. Briefly, the cement paste was prepared by manually mixing either the unground, ground, or coground reactive powders (DCPD and vaterite in equal amounts) with the liquid phase (deionized water) as previously published[33,34]; the L/S ratio was equal to 0.5 (w/w). In the present study, the paste prepared with unground reactive powders, that is, unground DCPD and unground vaterite (V1 or V2) is called the reference paste.

In the case of $SrCO_3$-loaded cements, various amounts of $SrCO_3$ were introduced in the solid phase (wt % of $SrCO_3$: 10, 15, or 20%) including the same weight ratio of vaterite 1 and DCPD (1:1) and the same L/S ratio as for the reference cement. The resulting cement paste contained 4, 6, or 8 wt % of Sr in the paste, respectively.

In all cases, the paste was then left setting in a sealed container at 37°C and in an atmosphere saturated with water ($\cong$100% humidity). The hardened and dried cement were analyzed after maturation during four days at 37°C.

Injectability measurement. Paste injectability was measured using a TAXT2 texture analyzer (Stable Micro Systems) equipped with a 25 kg load-cell carrier and a specific syringe system, including a 2.5-mL syringe (inner diameter of the syringe body = 9 mm and opening/exit diameter = 2 mm) without a needle.[19] We used a protocol designed to measure: (i) the force needed, expressed as the load (in kg), to apply on the piston to extrude a volume of paste corresponding to a displacement of 15 mm of the syringe piston at a constant rate of 2 mm/s (piston surface = 64 mm^2) and (ii) the weight of the paste extruded.

Briefly, each sample of paste (2 g of powder mixture and 1 g of deionized water) was prepared as described in section "Paste preparation." Measurements were performed at room temperature 5 min after the beginning of liquid and solid phase mixing ($t = 0$). This period (5 min) corresponds to the time needed to prepare the paste, introduce it within the syringe, and then leave it to rest for about 1 min before starting injectability measurements. This period can also correspond to the time a surgeon would need to prepare the cement paste and introduce it into a device for implantation by injection.

In addition, a balance was placed under the support of the syringe to weigh the amount of paste extruded at the end of the injection period. The extruded volume corresponding to a displacement of 15 mm of the syringe piston was chosen as large enough to minimize any difference in syringe geometry, which could hinder small differences between the samples. Each sample was analyzed at least in triplicate.

Paste homogeneity measurement: Filter-pressing determination. To identify and evaluate the phase separation ("filter-pressing") that occurred during paste extrusion using a syringe, we set a protocol to measure the weight of the paste extruded, the proportion of the solid phase in this paste, and the maximum load as a function of the position of the piston within the syringe.

We used the same equipment and conditions as for the injectability measurements (see section "Injectability measurement"). The only difference was that for each sample, we imposed three successive displacements of 5 mm for the piston instead of one displacement of 15 mm.

After each piston displacement, the paste extruded was weighed and then lyophilized to eliminate water. We also lyophilized the paste remaining within the syringe after 15 mm of piston-displacement. In all cases, the lyophilized powder was weighed, and the weight proportion of the solid phase in the paste was calculated from the two weighting. Each sample was tested at least in triplicate. Note that each lyophilized sample was thoroughly characterized by FTIR spectroscopy, scanning electron microscopy, and granulometry to check that the chemical reaction had not significantly begun (the powder components just after paste extrusion showed characteristics similar to those of the initial reactive powders).

Hardened cement physical–chemical characterization

Hardened cements prepared with unground, ground, and coground reactive powders were characterized using transmission FTIR spectroscopy from KBr pellets (Nicolet 5700 spectrometer, ThermoElectron), X-ray diffraction (Inel CPS 120 diffractometer) using a Co anticathode ($\lambda = 1.78897$ Å), and scanning electron microscopy (LEO 435 VP microscope; sample silver plating before observation).

The determination of the porosity of the cement was based on analyses performed in triplicate using a mercury intrusion porosimeter (Autopore IV 9400 Micromeritics® Instruments) with a 5-cm^3 solid penetrometer.

The compressive strength of the cement was evaluated using a Hounsfield Series S apparatus. The cement paste was placed in a cylindrical mould (diameter of 10.5 mm and height/diameter ratio $\cong$ 2) and packed tightly to eliminate any air bubbles trapped in the paste. After setting and hardening, the paste was placed in a sealed container saturated with water for 2 days at 37°C. The hardened cement was then withdrawn from the container and left to dry for 1 week at 37°C. The cement was removed from the mould and the compressive test performed.

Radio-opacity measurement

The radio-opacity of cement samples was measured in comparison with the optical density (OD) of a piece of aluminum of different thicknesses in accordance with ISO 9917-1

standard, which reports the method to determine the radio-opacity of dental hydraulic cements.

Cement pellets of 4 mm thick and 15 mm in diameter were prepared by molding the paste to be tested and then placing it in an atmosphere saturated with water and in an oven at 37°C. After cement setting and hardening, the pellets were removed from the mould and the radio-opacity measurements performed. These samples and a standard aluminum alloy (2017 A) step wedge were positioned side by side on a standard radiographic film (AGFA NDT D3 film with ultrafine grain). The aluminum wedge had a thickness ranging from 1 to 8 mm with a step of 0.5 mm. The step wedge served as an internal standard for each radiographic exposure and allowed the calculation of the radio-opacity of each sample in terms of aluminum thickness. Radiographic films were exposed for 6 or 7 s with a radioscopic X-ray system (Philips MG 103/2.25) at 65 kV and 10 mA. The focal distance between the X-ray tube and samples was 700 mm. The films were manually processed with appropriate chemicals (AGFA G135 developer and G335 fixer).

According to ISO 9917-1 standard, a cement will be 100% radio-opaque if its OD on X-ray radiography is equal to that of a piece of aluminum of the same thickness (i.e., 4 mm in our conditions).

The OD of the radiographic images of cement pellets and the aluminum wedge was measured with a portable transmission densitometer (X-Rite 331) using at least three readings per sample. The aluminum equivalence for each sample of cement was extrapolated to calculate the mean aluminum thickness equivalence. The radio-opacity (R) was calculated from the OD of the radiographic images of the cement pellet (OD_{cement}) and of the aluminum wedge (OD_{Al}) of the same thickness (i.e., 4 mm in the present study) by the following equation:

$$R = OD_{A1} \times 100/OD_{cement} \quad (1)$$

RESULTS

Characterization of powders

As we can see in Figure 1, the second protocol we set to prepare vaterite allowed us to obtain pure vaterite (V2). The particle size distributions of the two synthesized vaterite

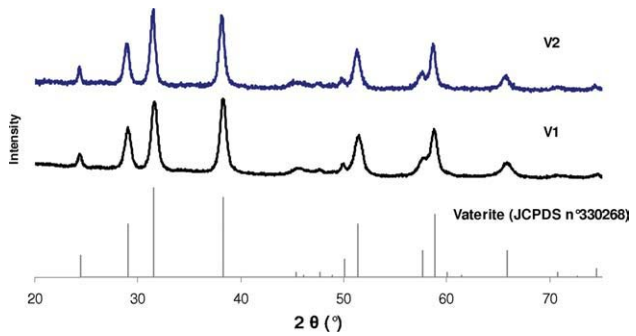

FIGURE 1. X-ray diffraction diagrams (Co anticathode, $\lambda = 1.78897$ Å) of the two vaterite powders synthesized (V1 and V2) and of vaterite from JCPDS data base. [Color figure can be viewed in the online issue, which is available at wileyonlinelibrary.com.]

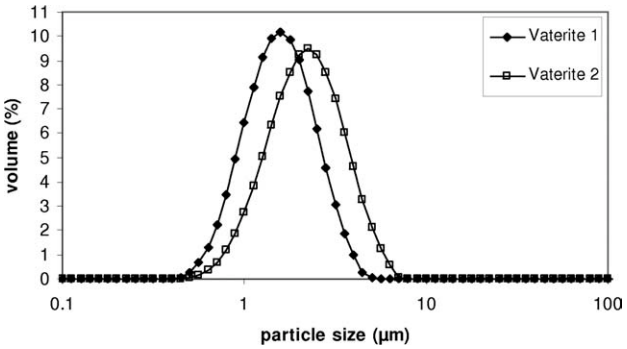

FIGURE 2. Particle size distribution of the synthesized V1 and V2.

powders are presented in Figure 2. In both cases, the particle size distribution is monomodal, and the mean diameter is equal to 1.7 ± 0.1 µm and 2.30 ± 0.03 µm for V1 and V2, respectively. The slower and controlled addition of the cationic solution during V2 synthesis could favor crystal growth and the formation of larger particles of vaterite. In addition, SEM analysis (Figure 3) shows larger agglomerates of vaterite particles for V2 compared to V1. Furthermore, we noted the different morphologies for these two vaterite samples: a lentil-like morphology for V1 and an oval or "flowers" morphology for V2 as described in other studies.[35]

When we coground the solid phase (DCPD and vaterite) including either V1 or V2, we see similar behaviors for both solid phases as a function of cogrinding time; a particle size limit of 2.7 µm is reached in both cases after 12 or 13 min of cogrinding (Figure 4).

Characterization of cement paste injectability

Figures 5 and 6 show the evolution of the load needed to extrude a given volume of paste, prepared with different solid phases, as a function of the position of the piston within the syringe. The values of the maximum load measured during piston displacement are reported in Table I.

We can see in Figure 5 that the reference pastes prepared either with V1 or V2 in the solid phase show similar injectability behaviors (maximum load around 33 kg). Furthermore, we observed a dramatic decrease in the load needed to extrude pastes prepared with ground DCPD in the solid phase. This decrease is higher when using V1 (maximum load = 5.5 kg) compared to V2 (maximum load = 20.0 kg). Figure 6 reveals that the injectability of the paste is even higher (lower load) when the solid phase is coground compared to components (DCPD) ground separately. If we examine Figures 5 and 6 and Table I, we can note that the maximum load needed to extrude the reference paste prepared with the (DCPD + V1) solid phase is almost divided by 100 when this solid phase is coground. In addition, we can clearly see that when ground or coground DCPD is associated with V2, the load is higher than when it is associated with V1 (Figures 5 and 6).

These injectability measurements can be correlated with the extruded paste weight measured after piston displacement was completed (Table I). As expected, we can see that the weight of the paste extruded increases when using

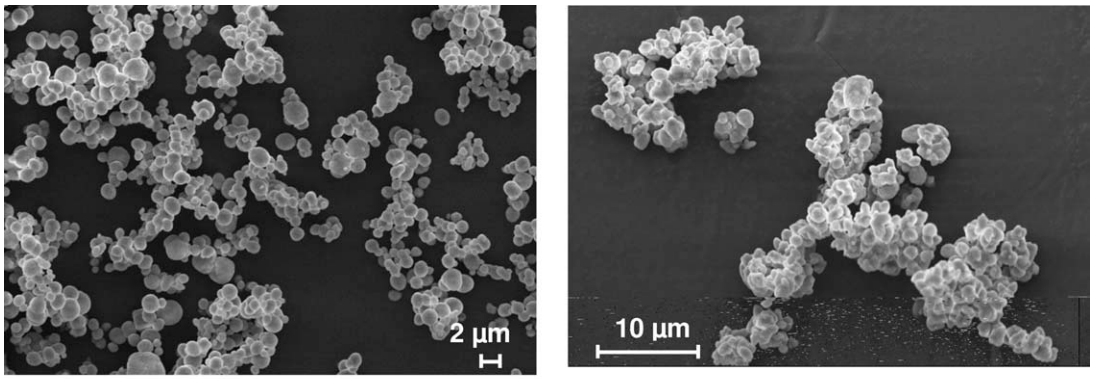

FIGURE 3. SEM micrographs of the two types of vaterite synthesized.

ground DCPD in the solid phase. This could be because of the increase in the density of the paste extruded or the decrease in filter-pressing or both.

Another important aspect of the curves presented in Figure 5 is the increase in the load as a function of piston displacement. This increase is marked, especially for both reference pastes (DCPD + V1) and (DCPD + V2), and appears less pronounced when ground DCPD is used in the solid phase. As already noted for the variation in the amount of paste extruded, this evolution could also be the result of filter-pressing often occurring for mineral cement paste, which undergoes a phase separation during extrusion. As a higher proportion of liquid is generally first extruded, the paste remaining in the syringe becomes thicker and thereby gradually harder to extrude.

Figure 6 reveals that cogrinding the solid phase allows the maintaining of a low and constant load to extrude the paste all along piston displacement.

Complementarily, we report in Figure 7 the measurements of the injectability of the paste prepared with the unground solid phase and with different L/S ratios (L/S = 0.52–1.01). As expected, injectability increases (reduced load) when the L/S ratio increases. In addition, we notice that the maximum load measured at the end of piston displacement reaches 14.6 and 0.5 kg for L/S = 0.75 and 1.01, respectively. These levels of injectability correspond to those measured for the paste prepared with ground DCPD and V2 and coground (DCPD + V2), respectively (Figures 5 and 6).

All these results show that grinding and cogrinding allow us to increase significantly paste injectability and reduce the L/S ratio. Another aspect that is now important to investigate is related to paste homogeneity and the possible phase separation that can occur during its extrusion.

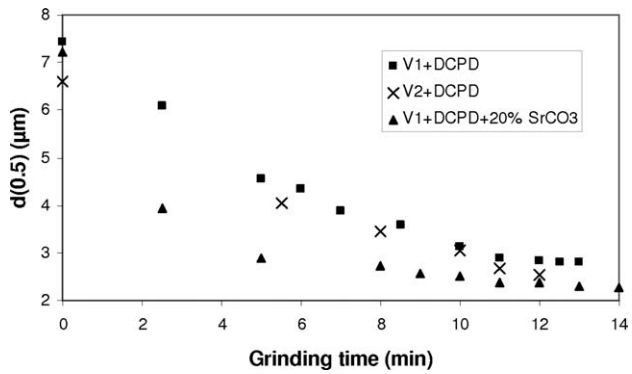

FIGURE 4. Evolution of the particle mean size of various coground solid phases as a function of grinding time.

Characterization of paste homogeneity

Figure 8(a,b) illustrates the results obtained using the protocol we set to evaluate filter-pressing. Figure 8(a) shows the evolution of the injectability of the reference paste as a function of piston position in the syringe body and of the piston displacement protocol used (15 mm in one step or 15 mm in three steps of 5 mm). We can see that for the rerun of piston, displacement at 5 and 10 mm involved in the three-step protocol, two additional millimeters were needed to recover the injectability rate of the paste obtained with the one-step protocol [see part of the curves unparallel in Figure 8(a)]. This observation could be related to the paste relaxation occurring when the piston stops after an intermediary step.

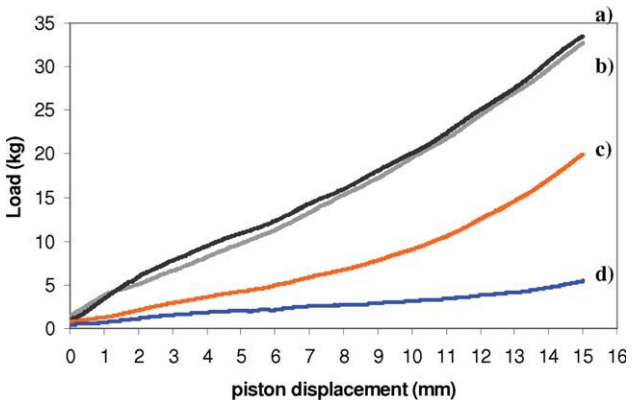

FIGURE 5. Measurement at room temperature of the load (in kg) applied on the piston to extrude the paste as a function of the syringe piston displacement: (a) unground DCPD + V1; (b) unground DCPD + V2; (c) ground DCPD + V2; and (d) ground DCPD + V1. [Color figure can be viewed in the online issue, which is available at wileyonlinelibrary.com.]

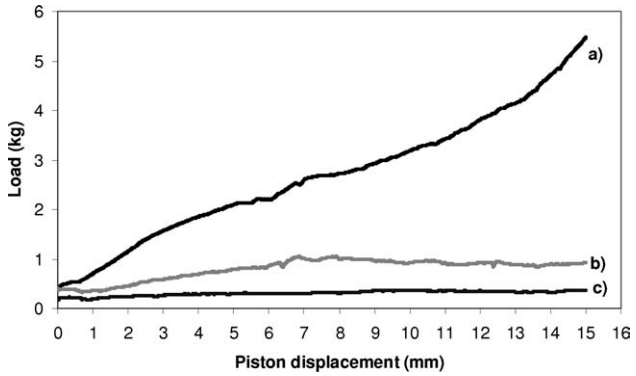

FIGURE 6. Measurement at room temperature of the load (in kg) applied on the piston to extrude the paste as a function of the syringe piston displacement: (a) ground DCPD + V1; (b) coground (DCPD + V2); and (c) coground (DCPD + V1).

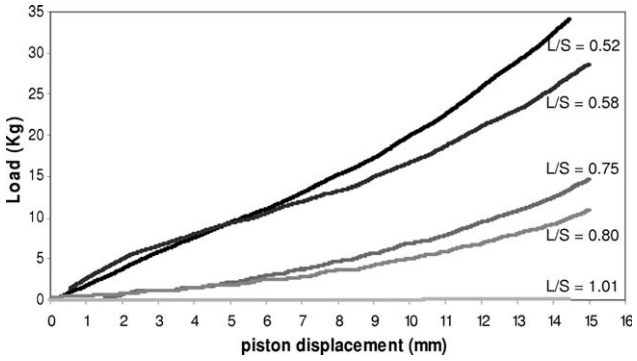

FIGURE 7. Influence of the *L*/*S* ratio on the load (in kg) to apply on the piston to extrude the reference paste at room temperature.

For the three-step protocol, the weight of the paste extruded, and the maximum load is reported in Table II as a function of piston position within the syringe. For the paste prepared with the unground solid phase, we notice that the successive steps of paste extrusion were associated with a decrease in the weight of the extruded paste and with an increase in the maximum load as the piston progressed. The increase of the maximum load was particularly high after 10 mm of piston displacement; this load reached 27 kg at 15 mm (Table II). However, when using the coground solid phase, the maximum load to extrude the paste was stable, especially during the first 10 mm of piston displacement; then, the variation was tiny for the last 5 mm of piston displacement. The maximum load reached 1.1 kg, which is far below that measured for the reference paste.

In addition to those in Table I, the results reported in Table II confirm that for the same L/S ratio the weight of the paste extruded when using the coground solid phase was dramatically higher than for the reference paste (unground solid phase), probably indicating the marked variation in solid fraction in the paste as the piston progresses.

To further investigate the possible variation in solid fraction in both pastes during extrusion, Figure 8(b) shows the evolution of the weight of the solid phase in each extruded paste sample as a function of piston position using a three-step protocol. For the reference paste, the weight proportion of the solid phase in the paste increases gradually (from 53 to 57% w/w) during piston displacement, whereas it is stable and significantly higher (around 64% w/w) for the paste prepared with the coground solid phase. Note that the latter is close to the expected value of solid proportion, that is, 67% w/w, corresponding to the initial paste composition (L/S ratio of 0.5). In addition, the weight proportion of the solid phase indicated at ">15 mm" [Figure 8(b)] corresponds to the composition of the paste remaining in the syringe body when the piston has stopped; it is around 64% w/w in both cases. These results clearly indicate that the reference paste first extruded contains a higher liquid proportion and that the remaining paste is progressively enriched in solid phase as piston displacement progresses, resulting in a dramatic augmentation of the load to extrude it. This evolution is no longer observed when using the coground solid phase.

However, it can be noted that a higher solid weight % would have been expected (>67%) for the reference paste remaining in the syringe after injectability test [>15 mm, Figure 8(b)]. The various tests performed at least in triplicate systematically lead to values lower than 67% letting us hypothesize that this issue is related to the protocol itself (difficulty in withdrawing all the solid from the syringe after lyophilization and before weighting etc.). We are currently investigating a refinement of this protocol to fix this issue.

Characterization of cement porosity and mechanical properties

The total porosity measured for the cement prepared with the unground, ground DCPD, or coground solid phase is around 60%. However, if we examine the pore size distribution presented in Figure 9, we can observe some differences. We note that the micropores of about 9 μm in diameter present in the reference cement have disappeared in the cement prepared with the ground or coground solid phase. In addition, nanosized pore distribution appears clearly as bimodal (10 and 18 nm) for the reference cement, whereas

TABLE I. Injectability Measurements (Maximum Load and Extruded Paste Weight Corresponding to 15-mm Piston Displacement) for Pastes Prepared With Different Solid Phases

Solid Phase Composition	DCPD + V2	DCPD + V1	Ground DCPD +V2	Ground DCPD + V1	Coground (DCPD + V2)	Coground (DCPD + V1)
Extruded paste weight (g)	1.01	1.03	1.25	1.44	1.51	1.54
Maximum load (kg)	32.7	33.5	20.0	5.5	1.0	0.4

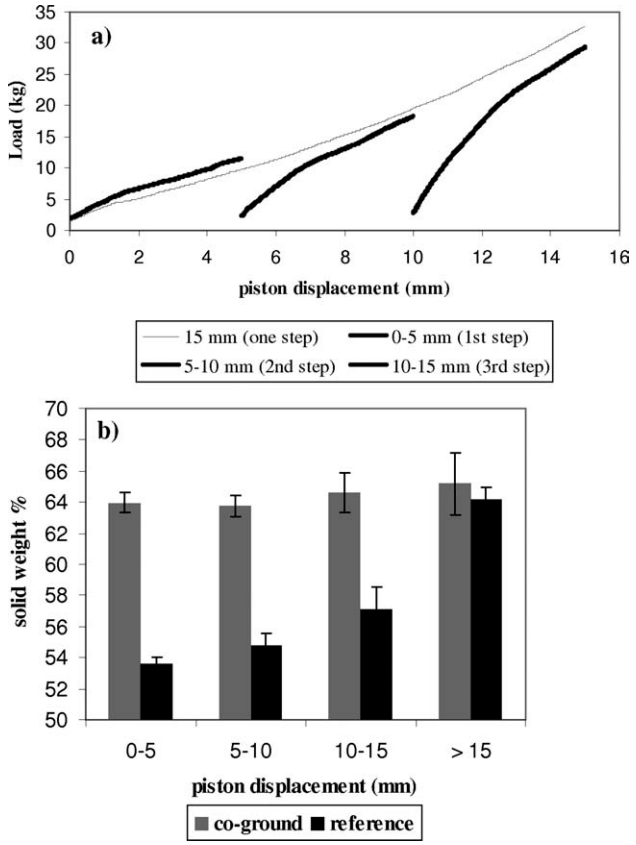

FIGURE 8. Filter-pressing evaluation: (a) measurement at room temperature of the load (in kg) applied on the piston to extrude the reference paste as a function of piston position within the syringe and piston displacement protocol (one step or three steps); and (b) proportion of solid phase within the extruded paste prepared with the reference or coground solid phase as a function of piston position within the syringe (from 0 to 5 mm, 5 to 10 mm, and 10 to 15 mm) and in the paste remaining within the syringe after 15 mm-piston-displacement.

it becomes monomodal (14 nm) for cements prepared with the solid phase including ground DCPD. Finally, we can see that this nanosized pore distribution is shifted toward lower pore dimensions (12 nm) in the case of cement prepared with the coground solid phase.

Additionally, we determined the compressive strength of the cements prepared with the different solid phases but equal L/S ratio, that is, 0.5 (Table III). Only a very slight increase of compressive strength can be noted when the solid phase is pretreated by grinding.

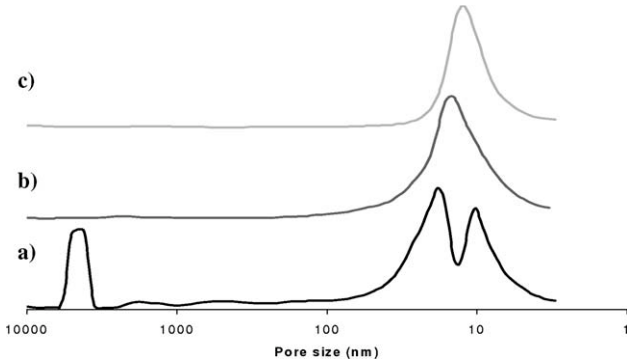

FIGURE 9. Pore size distribution for the cements after setting and hardening for one week at 37°C ($L/S = 0.5$): (a) reference cement (unground solid phase); (b) cement prepared with ground DCPD + V1; and (c) cement prepared with coground (DCPD + V1).

Addition of $SrCO_3$ and evaluation of cement radio-opacity

The addition of $SrCO_3$ in the cement solid phase was evaluated as a contrasting agent, and the cogrinding process was used to investigate its contribution in the control of cement radio-opacity.

The radiography of the different cement pellets presented in Figure 10 reveals the enhancement of the radio-opacity of the cement as a function of strontium carbonate load either in the unground or coground solid phase. If we thoroughly examine the radiography, we notice that for the same proportion of Sr (from 0 to 8% Sr w/w in the paste), the OD is uniform all over the cement pellets prepared with the coground solid phase. As a consequence, the latter shows an enhanced homogeneity and level of OD because of solid phase cogrinding treatment. For example, reference cements loaded with 4% of Sr show some isolated spots of high OD, probably because of the presence of $SrCO_3$ agglomerates, whereas in the case of cement prepared with the coground solid phase, the OD appears uniform because of the homogeneous distribution of $SrCO_3$ in the coground solid phase. This difference is less marked when a high proportion of $SrCO_3$ is used (e.g., for 8% Sr), because the amount of Sr introduced is high enough to be well distributed over the cement pellet with the simple manual mixing of the solid phase.

To determine the minimum amount of $SrCO_3$ to add into the cement solid phase to reach the radio-opacity required by ISO 9917-1 standard, we reported in Figure 11 the radio-opacity values calculated with Eq. (1) as a function of

TABLE II. Weight of Paste Extruded and Maximum Load Measured as a Function of the Piston Position for the Pastes Prepared With the Unground and Coground Solid Phase

	Paste Prepared With the Unground Solid Phase (Reference)		Paste Prepared With the Coground Solid Phase	
Piston Displacement (mm)	Weight of paste extruded (g)	Maximum load (kg)	Weight of paste extruded (g)	Maximum load (kg)
0–5	0.38 ± 0.01	11.2 ± 0.4	0.52 ± 0.01	0.7 ± 0.2
5–10	0.36 ± 0.03	17 ± 1	0.52 ± 0.01	0.7 ± 0.2
10–15	0.27 ± 0.02	27 ± 3	0.49 ± 0.03	1.1 ± 0.2

TABLE III. Compressive Strength of Hardened Cement (After 1 Week at 37°C) Prepared With Different Solid Phases

Solid Phase Composition	DCPD + V1	Ground DCPD + V1	Coground (DCPD + V1)
Compressive strength (MPa)	12 ± 1	16 ± 2	15 ± 3

the weight proportion of strontium in the paste. This figure shows that the radio-opacity of the reference cement (unground solid phase without Sr) is 55% (according to ISO 9917-1 standard) and increases linearly with the amount of Sr introduced into the cement. The examination of the relative positions of the values obtained in both cases (unground and coground solid phases) confirmed that cements prepared with the coground solid phase are slightly more radio-opaque than those prepared with the unground solid phase. In addition, we extrapolated a straight line in both cases and determined the theoretical values OF the amount of Sr to BE introduceD into the paste to reach a radio-opacity equal to that of a 4-mm thick Al wedge: 9.2 and 8.2% wt % of Sr for the paste prepared with unground and coground solid phases, respectively.

Finally, we evaluated the possible effect on the cement paste injectability of the addition of $SrCO_3$ powder into the solid phase. We can see in Figure 12 that whatever the proportion of strontium introduced into the coground solid phase, the injectability of the paste (0, 4, 6, or 8% of Sr) remains very high (maximum load for paste including 8% of Sr $<$ 0.4 kg) and constant all along piston displacement.

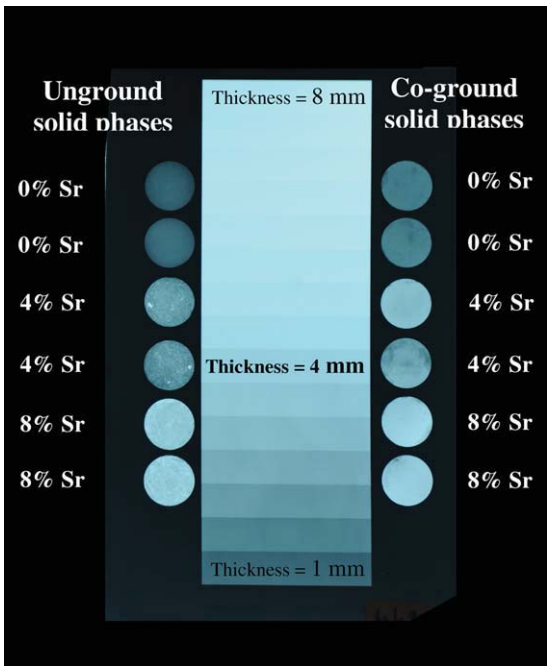

FIGURE 10. Radiography of standard aluminum alloy step wedge (in the center) and strontium-loaded cement pellets prepared with the unground solid phase (on the left) or coground solid phase (on the right). [Color figure can be viewed in the online issue, which is available at wileyonlinelibrary.com.]

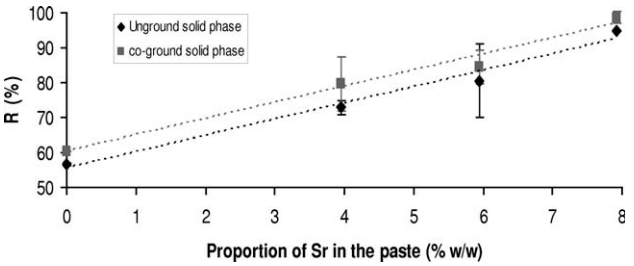

FIGURE 11. Influence of the weight proportion of strontium in the cement paste on the radio-opacity of cement (*R* in %) prepared with the unground solid phase or with coground solid phase.

The characterization of the commercial $SrCO_3$ powder used in this study showed that it is constituted of granular particles of a mean diameter of 9 μm (data not presented), which is in the range of that for DCPD particles. In addition, the evolution of the particle mean diameter of the solid phase including 20% w/w of $SrCO_3$ (corresponding to 8% w/w of Sr in the paste) during the cogrinding can be seen in Figure 4: up to 5 min of cogrinding, the decrease in the mean diameter of particles is faster to that observed for the unloaded solid phases (0% of Sr). Then, a size limit of 2.3 μm is reached after 13 min of cogrinding, which is close to that observed for the unloaded solid phases (2.7 μm).

These results show (i) that the addition of $SrCO_3$ powder in the solid phase does not significantly modify the behavior of the reactive powders during cogrinding and leads to a paste with similar injectability property; (ii) the efficiency of the cogrinding process in controlling mixed powder association, particles size, and, consequently, the injectability of the paste even in the case of solid phase including three powder components.

DISCUSSION

Injectability and homogeneity of the paste

The results presented in Figures 5 and 6 reveal the improvement of the injectability of the paste when DCPD is ground, especially when the solid phase is coground. It is

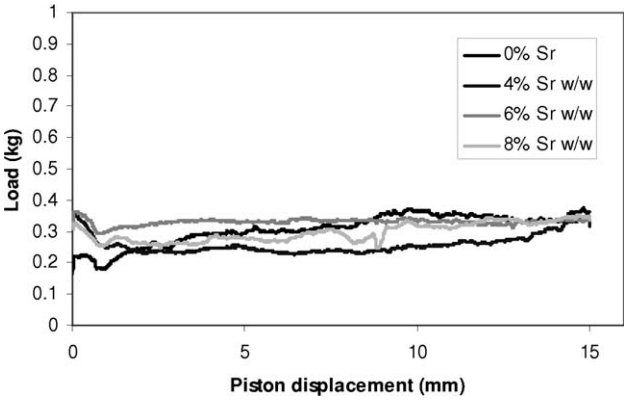

FIGURE 12. Measurement at room temperature of the load (in kg) applied on the piston to extrude strontium-loaded cement paste as a function of the syringe piston displacement and of the % of Sr introduced into the paste, that is, in the coground solid phase.

interesting to note that the two types of reference paste, prepared either with the (DCPD + V1) or (DCPD + V2) solid phase, show the same injectability (see curves a and b in Figure 5) behavior, which goes against what is generally found in the literature, that is, particle size and agglomeration state are key factors controlling paste injectability.[18,21] However, when DCPD powder is preground for 27 min, the type of vaterite introduced into the solid phase has a significant effect on paste injectability: the maximum load reaches 20 kg with V2 and 5.5 kg with V1 (see curves c and d in Figure 5). These results reveal the major role of unground DCPD particles, which are the limiting parameters for paste extrusion because of their morphology (platelet) and large dimensions (d_{50} = 9.2 ± 0.3 μm[33]), impairing piston displacement. However, when DCPD particles are ground, thereby reaching a mean particle size of 2.7 μm and presenting more isotropic particle morphology, that is, close to that of vaterite particles (1.7 and 2.3 μm for V1 and V2, respectively), then the vaterite particle characteristics (particle size and agglomeration state) are the limiting parameters for paste extrusion. If we go further and examine Figures 5 and 6, we can see that the choice of the type of vaterite is less determining when the solid phase is coground than when only DCPD is ground (comparison of the curves c and d in Figure 5 and curves b and c in Figure 6). In addition, the low maximum load (0.4 kg), even for strontium-loaded cement paste and the horizontal curve obtained for paste prepared with the coground (DCPD + V1) or (DCPD + V1 + $SrCO_3$) solid phase (Figures 6 and 12) confirm the benefit of solid phase cogrinding treatment.

Another important parameter that controls cement properties is the L/S ratio. We have shown that when using the cogrinding treatment of the solid phase and an L/S ratio of 0.5, we can reach the same injectability as that obtained for the reference paste (unground solid phase) prepared with an L/S ratio of 1.01 (comparison of Figures 6 and 7). It is well known that lowering the L/S ratio allows achieving better mechanical properties of cements.[3,15] In addition, recently, we have shown that $CaCO_3$-DCPD cement setting time is nearly halved when using the coground solid phase.[33] The decrease in setting time and the higher and controlled injectability point out the determining and promising role of the cogrinding process to meet a surgeon's requirements for such injectable cements. As reported by several authors, a compromise between good injectability, fast setting, and mechanical properties has always to be sought. Interestingly, the results reported by Tadier et al. in part I[33] and in the present study reveal that the cogrinding process allows optimizing all these paste and cement properties (decrease of setting time, increase of injectability and mechanical properties) and involves processing parameters (cogrinding duration, etc.) that are adaptable to the industrial development of cements.

Finally, it is important to note that for each sample, the shape of the injectability curve, the load level measured, and the amount of paste extruded are repeatable, which confirms the reliability of the specific syringe system and protocol set used to evaluate the injectability of this self-setting paste.[19]

We have shown that an increase in paste injectability is also associated with an increase in the extruded paste weight (Table II). Moreover, it was important to evaluate the possible phase separation during cement paste extrusion, which remains the main phenomenon leading to poor injectability of bone mineral cements.[36] Some analogies can be noted between our protocol and the protocol Habib et al. used for the study of phase separation of a nonsetting calcium phosphate paste.[8,36] In the case of $CaCO_3$-DCPD self-setting paste, our results confirmed that filter-pressing no longer occurs during paste extrusion when the solid phase is coground. Indeed, the increase in the load observed on the injectability curves for nontreated reactive powders or solid phase is related to the increase in the amount of solid plug at the syringe nozzle, which progressively prevents the paste from extruding. We have also shown that the proportion of solids (64% w/w) in the paste prepared with the coground solid phase is close to that in the initial paste (67% w/w) prepared with L/S = 0.5, confirming the absence of phase separation (filter-pressing) in the paste when the solid phase is coground. This result can also be checked when examining the aspect of the reference paste extruded, which seems to be heterogeneous and segmented compared to the continuous and homogeneous "spaghetti" of paste obtained after extrusion when using the coground solid phase (data not presented).

It is of prime importance to avoid filter-pressing to control the composition of the extruded paste and, consequently, the composition of the cement implanted *in vivo*. We have shown that the cogrinding process can contribute significantly to this requirement.

Porosity and mechanical properties of the cement

Cement porosity is a key parameter for resorbable cements, because it controls not only the mechanical properties of the cement but also its biological properties. Ginebra et al.[22] showed that a decreasing particle size of the reactive powder (α tricalcium phosphate) increases the number of contacts between the particles, which in turn leads to the decrease in cement porosity. In the case of amorphous calcium phosphate-DCPD cement, a dramatic decrease in cement total porosity was found by Tofighi et al.[37] when combining 24 h of grinding solid phase pre-treatment and a decrease of the L/S ratio.

In the present study, porosimetry analysis revealed the disappearance of pore sizes of around 9 μm in diameter in hardened cement prepared with the coground solid phase. Interestingly, this size corresponds to the dimension of unground DCPD crystals (9.2 ± 0.3 μm).[33] We can hypothesize that the dissolution of large unground DCPD platelets during cement setting reaction could leave an empty space, thereby creating the reference cement microporosity. The SEM micrograph of a hardened reference cement presented in Figure 13 revealed the presence of some thin elongated micropores with dimension similar to that of unground DCPD platelet crystals.[33] When the solid phase is coground, the DCPD particles are smaller and intimately associated with vaterite particles,[33] which in turn lead to a lower and

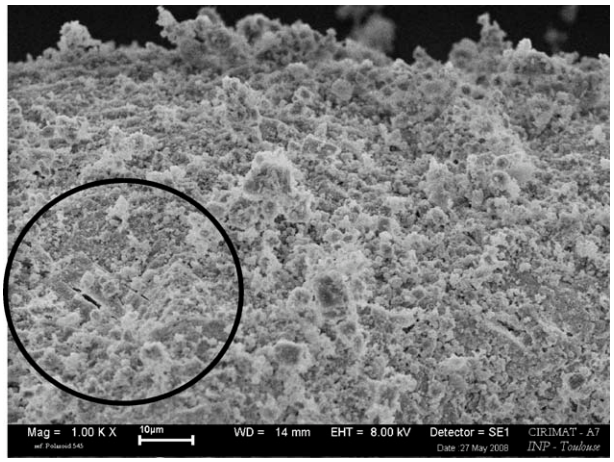

FIGURE 13. SEM micrograph of a set reference cement. The black circle highlights the presence of pores with dimension and form similar to unground DCPD platelet crystals.

more homogeneously distributed pore size (monomodal pore size distribution, Figure 9); however, we also showed that cement total porosity remains constant, probably because of the constant L/S ratio used to prepare the paste.

The effect of the solid phase cogrinding on the cement's mechanical properties is also limited (small increase in compressive strength, Table III). However, we showed that cogrinding the solid phase allows reaching earlier good paste resistance (shorter setting time).[33] In addition, the mechanical properties can be enhanced by optimizing the L/S ratio; this ratio can be decreased when using the coground solid phase because of the lower plastic limit, which corresponds to the minimum amount of liquid to be added to a powder to form a paste. However, several parameters related to the solid phase particle size distribution and specific surface area are involved in the variation of the plastic limit, and it seems difficult to determine their contribution and, consequently, that of the cogrinding process.[13]

For example, we observed a significant increase in cement's mechanical properties, for cement prepared with the coground solid phase and an L/S ratio of 0.44 instead of 0.5: $R_{comp} = 19 \pm 3$ MPa. However, a compromise must be found, because a decrease in the L/S ratio leads to a decrease in cement paste injectability (Figure 5).

Cement radio-opacity and Sr addition

This study shows that cement radio-opacity increased linearly as a function of strontium proportion in the cement, thereby pointing out the efficiency of strontium as a contrast agent and confirming the results obtained by Wang et al.[26]

In the present study, several parameters can contribute to this enhancement of cement radio-opacity including (i) the presence of strontium, which has a higher atomic number than other elements present in the cement; and (ii) the homogeneous distribution of Sr within the cement owing to the cogrinding treatment. In this study, strontium plays the role of contrasting agent and marker of cement homogeneity; it points out the synergistic effect of the cogrinding process, which enhances homogeneity and, consequently, the radio-opacity of unloaded or Sr-loaded cements.

In addition, with the coground solid phase loaded with strontium, we can expect to further optimize the radio-opacity of the cement by decreasing the L/S ratio and thereby the proportion of Sr to be introduced into the paste ($\leq$8.2% of Sr in the paste). It is important to control the amount of strontium in the cement, because it has been shown that it has a synergistic positive effect on bone formation by stimulating osteoblast cells and inhibiting osteoclasts[31]; however, it has also been reported that large doses of strontium can have a negative effect on bone formation.[32] The release properties of the as-prepared Sr-loaded cements will be presented in another work.

CONCLUSION

The new protocol we set to synthesize vaterite led to pure vaterite powder (V2) with different particle characteristics (size, morphology, and agglomeration state) than those of vaterite powder (V1) synthesized with the protocol previously published[33,34]; we showed that these vaterite features have a determining role on paste injectability when associated with ground DCPD.

This study showed that the cogrinding treatment of the solid phase leads to synergistic positive effects on several properties of $CaCO_3$-DCPD cement prepared with the same L/S ratio:

i. It allows maintaining a low and constant load (<0.4 kg) to extrude the paste all along piston displacement. Analogous behavior has been observed when a third component ($SrCO_3$) is added into the solid phase.
ii. It allows maintaining the solid weight proportion of the extruded paste close to that in the initial paste all along piston displacement. This homogeneity of the paste was demonstrated using the quantitative and discriminating protocol we set to evaluate filter-pressing. The enhancement of the homogeneity of the hardened cement was confirmed by the addition of strontium completed by OD measurements; the latter have allowed us to determine the minimum amount of strontium to add into the cement paste to reach the radio-opacity required by ISO 9917-1 standard.
iii. It affects the pore size distribution but not the total porosity of the hardened cement.

Interestingly, this study reveals that the cogrinding process allows optimizing several paste and cement properties (increase of injectability, mechanical properties, and radio-opacity) and controlling the solid fraction in the extruded paste. It involves processing parameters (cogrinding duration) that could be easily scaled up. This constitutes a decisive advantage for the development of $CaCO_3$-DCPD cements and, more generally, multicomponent injectable bone cements that meet a surgeon's requirements.

REFERENCES

1. Lewis G. Injectable bone cements for use in verteobroplasty and kyphoplasty: State-of-the-art review. J Biomed Mater Res B: Appl Biomater 2006;76:456–468.

2. Bohner M. Calcium orthophosphates in medicine: From ceramics to calcium phosphate cements. Injury Int J Care Injured 2000; 31(Suppl 4):37–47.
3. Dorozhkin S. Calcium orthophosphates cements and concretes. Materials 2009;2:221–291.
4. Bohner M, Gbureck U, Barralet JE. Technological issues for the development of more efficient calcium phosphate bone cements: A critical assessment. Biomaterials 2005;26:6423–6429.
5. Khairoun I, Driessens FCM, Boltong MG, Planell JA, Wenz R. Addition of cohesion promotors to calcium phosphate cements. Biomaterials 1999;20:393–398.
6. Takechi M, Ishikawa K, Miyamoto Y, Nagayama M, Suzuki K. Tissue responses to anti-washout apatite cement using chitosan when implanted in the rat tibia. J Mater Sci: Mater Med 2001;12:597–602.
7. Wang X, Chen L, Xiang H, Ye J. Influence of anti-washout agents on the rheological properties and injectability of a calcium phosphate cement. J Biomed Mater Res B: Appl Biomater 2007;81: 410–418.
8. Habib M, Baroud G, Gitzhofer F, Bohner M. Mechanisms underlying the limited injectability of hydraulic calcium phosphate paste. Acta Biomater 2008;4:1465–1471.
9. Xu HHK, Takagi S, Quinn JB, Chow LC. Fast-setting calcium phosphate scaffolds with tailored macropore formation rates for bone regeneration. J Biomed Mater Res A 2004;68:725–734.
10. Bohner M, Doebelin N, Baroud G. Theoretical and experimental approach to test the cohesion of calcium phosphate pastes. Eur Cells Mater 2006;12:26–35.
11. Wang X, Ye J, Xiang H. Effect of additives on the rheological properties and injectability of a calcium phosphate bone substitute material. J Biomed Mater Res B: Appl Biomater 2006;78:259–264.
12. Leroux L, Hatim Z, Frèche M, Lacout JL. Effects of various adjuvants (lactic acid, glycerol, and chitosan) on the injectability of a calcium phosphate cement. Bone 1999;25:31S–34S.
13. Bohner M, Baroud G. Injectability of calcium phosphate pastes. Biomaterials 2005;26:1553–1563.
14. Ginebra MP, Rilliard A, Fernández E, Elvira C, San Román J, Planell JA. Mechanical and rheological improvement of a calcium phosphate cement by the addition of a polymeric drug. J Biomed Mater Res 2001;57:113–118.
15. Burguera EF, Xu HHK, Sun L. Injectable calcium phosphate cement: Effects of powder-to-liquid ratio and needle size. J Biomed Mater Res B: Appl Biomater 2008;84:493–502.
16. Gbureck U, Spatz K, Thull R, Barralet JE. Rheological enhancement of mechanically activated α-tricalcium phosphate cements. J Biomed Mater Res B: Appl Biomater 2005;73:1–6.
17. Khairoun I, Boltong MG, Driessens FCM, Planell JA. Some factors controlling the injectability of calcium phosphate bone cements. J Mater Sci Mater Med 1998;9:425–428.
18. Baroud G, Cayer E, Bohner M. Rheological characterization of concentrated aqueous β-tricalcium phosphate suspensions: The effect of liquid-to-powder ratio, milling time, and additives. Acta Biomater 2005;1:357–363.
19. Combes C, Tadier S, Galliard H, Girod-Fullana S, Charvillat C, Rey C, Auzély-Velty R, El Kissi N. Rheological properties of calcium carbonate self-setting injectable paste. Acta Biomater 2010;6: 920–927.
20. Tadier S, Le Bolay N, Girod Fullana S, Rey C, Combes C. Control of the injectability of calcium carbonate-calcium phosphate mixed cements for bone reconstruction. Key Eng Mater 2009;396–398: 225–228.
21. Delgado JA, Harr I, Almirall A, del Valle S, Planell JA, Ginebra MP. Injectability of a macroporous calcium phosphate cement. Key Eng Mater 2005;284–286:157–160.
22. Ginebra MP, Driessens FCM, Planell JA. Effect of the particle size on the micro and nanostructural features of a calcium phosphate cement: A kinetic analysis. Biomaterials 2004;25:3453–3462.
23. Liu C, Shao H, Chen F, Zheng H. Rheological properties of concentrated aqueous injectable calcium phosphate cement slurry. Biomaterials 2006;27:5003–5013.
24. Hernández L, Gurruchaga M, Goñi I. Influence of powder particle size distribution on complex viscosity and other properties of acrylic bone cement for vertebroplasty and kyphoplasty. J Biomed Mater Res B: Appl Biomater 2006;77:98–103.
25. Gbureck U, Barralet JE, Spatz K, Grover LM, Thull R. Ionic modification of calcium phosphate cement viscosity, Part 1: Hypodermic injection and strength improvement of apatite cement. Biomaterials 2004;25:2187–2195.
26. Wang X, Ye J, Wang Y. Influence of a novel radiopacifier on the properties of an injectable calcium phosphate cement. Acta Biomater 2007;3:757–763.
27. Romieu G, Garric X, Munier S, Vert M, Boudeville P. Calcium-strontium mixed phosphate as novel injectable and radio-opaque hydraulic cement. Acta Biomater 2010;6:3208–3215.
28. Alkhraisat MH, Marino FT, Rodriguez CR, Jerez LB, Lopez-Carbacos E. Combined effect of strontium and pyrophosphate on the properties of brushite cements. Acta Biomater 2008:4;664–670.
29. Guo D, Xu K, Zhao X, Han Y. Development of a strontium-containing hydroxyapatite bone cement. Biomaterials 2005;26:4073–4083.
30. Pina S, Torres PM, Goetz-Neunhoeffer F, Neubauer J, Ferreira JMF. Newly developed Sr-substituted α-TCP bone cements. Acta Biomater 2010;6:928–935.
31. Marie PJ, Ammann P, Boivin G, Rey C. Mechanisms of action and therapeutic potential of strontium in bone. Calc Tissue Int 2001; 69:121–129.
32. Cohen-Solal M. Strontium overload and toxicity: Impact on renal osteodystrophy. Nephrolgy Dial Transpl 2002;17:30–34.
33. Tadier S, Le Bolay N, Rey C, Combes C. Co-grinding significance for calcium carbonate-calcium phosphate mixed cement, Part 1: Effect of particle size and mixing on solid phase reactivity. Acta Biomater 2011;7:1817–1826.
34. Combes C, Bareille R, Rey C. Calcium carbonate-calcium phosphate mixed cement compositions for bone reconstruction. J Biomed Mater Res 2006;79:318–328.
35. Yan G, Wang L, Huang J. The crystallization behaviour of calcium carbonate in ethanol/water solution containing mixed non-ionic/anionic surfactants. Powder Technol 2009;192:58–64.
36. Habib M, Baroud G, Gitzhofer F, Bohner M. Mechanisms underlying the limited injectability of hydraulic calcium phosphate paste, Part 2: Particle separation study. Acta Biomater 2010;6:250–256.
37. Tofighi A, Palazzolo R. Calcium phosphate bone cement preparation using mechano-chemical process. Key Eng Mater 2006; 284–286:101–104.